

**Direct observation of site-specific valence electronic structure at the SiO<sub>2</sub>/Si interface**Y. Yamashita,<sup>1,\*</sup> S. Yamamoto,<sup>1</sup> K. Mukai,<sup>1</sup> J. Yoshinobu,<sup>1</sup> Y. Harada,<sup>2</sup> T. Tokushima,<sup>2</sup> T. Takeuchi,<sup>2</sup> Y. Takata,<sup>2</sup> S. Shin,<sup>1,2</sup> K. Akagi,<sup>3</sup> and S. Tsuneyuki<sup>3</sup><sup>1</sup>*The Institute for Solid State Physics, The University of Tokyo, Kashiwa, Chiba 277-8581, Japan*<sup>2</sup>*Riken/SPring-8, Sayo-gun, Hyogo 679-5148, Japan*<sup>3</sup>*Department of Physics, Graduate School of Science, The University of Tokyo, Bunkyo-ku, Tokyo 113-0033, Japan*

(Received 22 November 2005; published 31 January 2006)

Atom specific valence electronic structures at the solid-solid interface are elucidated successfully using soft x-ray absorption and emission spectroscopy. In order to demonstrate the versatility of this method, we investigated the SiO<sub>2</sub>/Si interface as a prototype and directly observed valence electronic states projected at the particular atoms of the SiO<sub>2</sub>/Si interface; the local electronic structure strongly depends on the chemical states of each atom. In addition, we compared the experimental results with first-principles calculations, which quantitatively revealed the interface properties in atomic scale.

DOI: [10.1103/PhysRevB.73.045336](https://doi.org/10.1103/PhysRevB.73.045336)

PACS number(s): 73.20.At, 68.35.Ct, 79.60.Jv

**I. INTRODUCTION**

Interfaces change the atomic structures and chemical compositions of matter, providing not only fascinating physical properties such as metal-insulator transition,<sup>1</sup> band gap narrowing,<sup>2</sup> and superconductivity<sup>3</sup> but also affecting the electronic properties of semiconductor devices.<sup>4</sup> Therefore, observing valence and/or conduction electronic states projected at an individual atom of the interface is in particular important to obtain an atom-based picture of physical properties of matter. In spite of many studies on interfaces, the interface electronic states have been evaluated mostly as average rather than individual states. Thus, we require a method that allows us to probe atom-specific electronic states directly at the interfaces.

Soft x-ray absorption (SXA) spectroscopy<sup>5</sup> is a method to study an excitation from a core level to conduction states, providing element-specific conduction states. Soft x-ray emission (SXE) spectroscopy<sup>6,7</sup> probes a photon emission process involving a core hole decay process predominantly from valence states to a core-level state, which addresses valence states of a particular atom. Moreover, since core electrons are localized to the particular atom, we can study the valence and conduction states in an atom-specific way using SXA and SXE spectroscopy. Thus, the selective photoabsorption at interfaces is realized by tuning the incident photon energy to only allow the electronic excitation from a core level to conduction band levels, using SXA. Once the core level at the interfaces is excited, the core hole is filled by an electron from an occupied valence level accompanied with soft X-ray emission. We thus have a tool to look into the nature of atom-specific occupied electronic states directly at the interface.

In this paper, we report direct observation of the valence electronic structure projected at a particular atom of the SiO<sub>2</sub>/Si interface using SXA and SXE spectroscopy. The local electronic states are noticeably different from those of bulk SiO<sub>2</sub> and are strongly dominated by the chemical states of each atom at the interface. Furthermore, we compare the experimental results with first-principles density functional calculations, which quantitatively reveal not only the Si-O-Si

bond angle and Si-O bond length at the interface but the interfacial electronic properties in atomic-scale.

**II. EXPERIMENT**

SiO<sub>2</sub>/Si(111) samples were prepared from phosphorus-doped *n*-type Si(111) wafers with a resistivity of 0.001 Ω cm. After standard RCA cleaning, a native oxide layer was etched away by a 1% HF solution and the wafers were then immersed in a 40% NH<sub>4</sub>F solution for 15 min to form an atomically smooth silicon surface [Si(111)(1×1)-H]. A 1.8 nm oxide layer was prepared in 0.1 M Pa of oxygen at 600 K for 5 min. It is noteworthy that the prepared oxide layer has an atomically smooth interface.<sup>8</sup>

The synchrotron radiation experiments were performed using BL-27SU at SPring8 with the approval of JASRI as a Nanotechnology Support Project (Proposal No. 2003B0209-Nsa-np-Na and 2004A0345-Nsa-np-Na). The oxygen *K*-edge absorption spectra were measured by detecting O *KVV* Auger electrons at 510 eV and an instrumental energy resolution of 50 meV. SXE spectroscopy was performed with an 800 meV energy resolution. The design and performance of the SXE spectrometer are described in detail elsewhere.<sup>9</sup>

First-principles calculations based on the density functional theory with a generalized gradient approximated correction were performed to evaluate the local density of states of the valence level and the interface structure and properties.<sup>10</sup> A six Si-layer thick slab model was used with a periodic boundary condition: The unit cell contains four dangling bonds of a clean Si(111) surface in its initial configuration. The oxidized structures were then obtained by inserting O atoms in series with structure relaxation. We prepared three models obtained through a different insertion order of oxygen atoms and adopted the most relaxed one.

**III. RESULTS AND DISCUSSION**

Figures 1(a) and 1(b) show the oxygen *K*-edge absorption spectra of SiO<sub>2</sub>/Si(111) structures with 1.8 nm and 8 nm thick SiO<sub>2</sub> layers, respectively. The latter is considered to

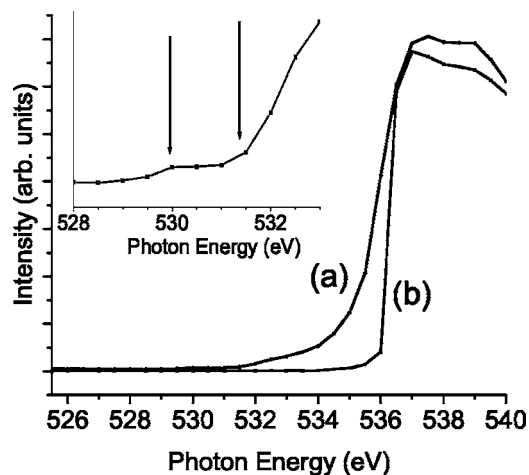


FIG. 1. Oxygen  $K$ -edge absorption spectra of (a) 1.8 nm thick  $\text{SiO}_2/\text{Si}(111)$  and (b) 8 nm thick  $\text{SiO}_2/\text{Si}(111)$  structures. The inset shows the magnified spectrum of (a). The incident photon angle was  $36^\circ$  from surface normal and  $p$ -polarized light was used. The Auger electrons were detected at the take off angle of  $54^\circ$ . Note that absorption from  $\text{O } 1s$  orbital to  $\text{O } 2s$  orbital is forbidden due to selection rules. Thus, these absorption spectra represent unoccupied  $\text{O } 2p$  states.

represent the bulk  $\text{SiO}_2$  spectrum since the mean-free path of the Auger electron is  $\sim 1.5$  nm at 510 eV,<sup>11</sup> which is much shorter than the  $\text{SiO}_2$  layer thickness. The absorption spectrum of the 1.8 nm thick  $\text{SiO}_2/\text{Si}(111)$  structure is strikingly different from the bulk  $\text{SiO}_2$  spectrum. The spectrum has a lower onset with the edge structures at 530 and 531.5 eV (see the inset of Fig. 1). Muller *et al.*<sup>12</sup> used electron energy loss spectroscopy and reported that the oxygen  $K$ -edge was lowered by 3 eV at the interface compared to the bulk  $\text{SiO}_2$ .<sup>12</sup> Thus, the edge structures in the spectrum are attributed to unoccupied  $\text{O } 2p$  states at the interface, and the lowered edge exhibits a reduced band gap at the interface. Note that the peak at 537.5 eV is due to unoccupied  $\text{O } 2p$  states that are hybridized with  $\text{Si } 3s$  and  $3p$  states of bulk  $\text{SiO}_2$ .<sup>13,14</sup>

As for the interface structure of  $\text{SiO}_2/\text{Si}$ , it is well known that the interface consists of intermediate oxidation states (namely suboxide), i.e.,  $\text{Si}^{1+}$  ( $\text{Si}_2\text{O}$ ),  $\text{Si}^{2+}$  ( $\text{SiO}$ ), and  $\text{Si}^{3+}$  ( $\text{Si}_2\text{O}_3$ ).<sup>8,15,16</sup> Analysis of the  $\text{Si } 2p$  photoelectron spectra for the 1.8 nm thick  $\text{SiO}_2/\text{Si}(111)$  indicates that the interface predominantly consists of  $\text{Si}^{1+}$  and  $\text{Si}^{3+}$  and the relative intensity of  $\text{Si}^{2+}$  is only 3%. This is consistent with the previous results.<sup>8</sup> According to the theoretical studies by Wallis *et al.*,<sup>17</sup> the oxygen  $K$  edge of the intermediate states in the amorphous silicon shifts to lower energy as the oxidation number of the adjacent silicon atoms decreases. Thus, we assigned the absorption edges at 530 and 531.5 eV to an  $\text{O}$  atom bonding to  $\text{Si}^{1+}$  and  $\text{Si}^{3+}$  at the interface, respectively (hereafter, we denote the  $\text{O}$  atom bonding to  $\text{Si}^{1+}$  and  $\text{Si}^{3+}$  at the interface as P1 and P3, respectively). Accordingly, a site-specific SXE spectrum of a particular oxygen atoms at the interface could be selectively obtained using different excitation energies, i.e., 530 eV for P1 and 531.5 eV for P3.

Figures 2(a)–2(c) show the  $\text{O } K$ -edge SXE spectra for the 1.8 nm thick  $\text{SiO}_2/\text{Si}(111)$  structure. The electronic states at

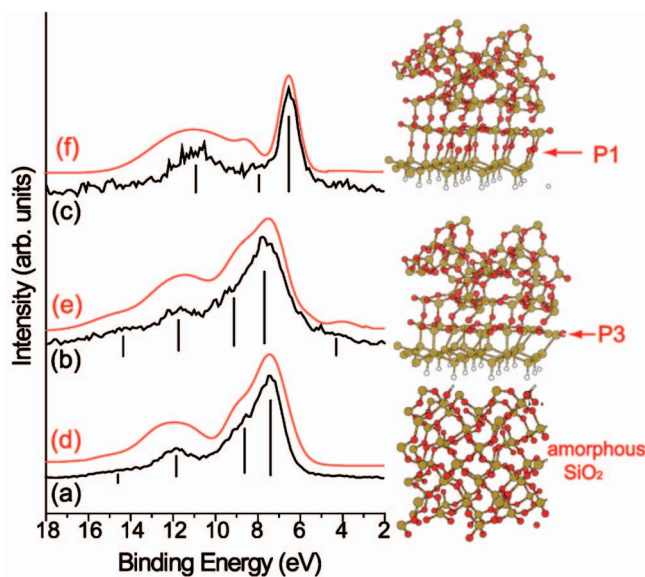


FIG. 2. (Color)  $\text{O } K$ -edge SXE spectra for the 1.8 nm thick  $\text{SiO}_2/\text{Si}(111)$  structure and the calculated  $\text{O } 2p$  DOS obtained from the model presented in this figure. For the SXE spectra shown as the black lines, incident photon energies were (a) 537.5 eV, (b) 533 eV, and (c) 530 eV. The incident photon angle was  $60^\circ$  from the surface normal and a  $p$ -polarized light was used. Note that in order to selectively excite P3, we used 533 eV as the incident light energy. Red lines show the calculated  $\text{O } 2p$  DOS for (d)  $\text{SiO}_2$ , (e) P3 atoms of  $\text{SiO}_2/\text{Si}(111)$  interface with P3, and (f) P1 atoms of  $\text{SiO}_2/\text{Si}(111)$  interface with P1. The calculated DOS spectrum was the average of each oxygen atom spectrum for amorphous  $\text{SiO}_2$  and that of each interface oxygen atom spectrum in the case of P1 and P3. Gaussian broadening was applied for the  $\text{O } 2p$  DOS using experimental and lifetime broadening (total 1.1 eV). Red and yellow balls correspond to oxygen and silicon atoms, respectively.

the interface are noticeably different from those of bulk  $\text{SiO}_2$  and the interfacial electronic states strongly depend on the intermediate oxidation states at the interface. With photon energy of 537.5 eV, the occupied  $\text{O } 2p$  states of bulk  $\text{SiO}_2$  predominantly contribute to the SXE spectrum [Fig. 2(a)]. In this spectrum, the peak at 7.25 eV and the shoulder at 8.65 eV are attributed to the  $\text{O } 2p$  nonbonding states, while the peaks at 11.75 and 14.33 eV are due to the bonding states between  $\text{O } 2p$  and  $\text{Si } sp^3$  orbitals.<sup>18</sup> When the incident photon energy is 533 eV in order to excite P3 [Fig. 2(b)], the peaks due to nonbonding states become broader and shift toward a higher binding energy compared to bulk  $\text{SiO}_2$ . In addition, a small peak around 4 eV is observed. By exciting P1 [Fig. 2(c)], the peak at 6.50 eV, which is attributed to the nonbonding states of  $\text{O } 2p$ , is very sharp, indicating a localized nonbonding state. The sharp peak might be attributed to resonant inelastic scattering.<sup>6</sup> An inelastic scattering peak should shift its energy position as a function of incident photon energy.<sup>6</sup> However, the peak position did not change with changing incident photon energy.

In order to quantitatively evaluate the interface states, the experimental results are directly compared with theoretical calculations, which provides atomic-scale information on the interface properties. For the  $\text{SiO}_2/\text{Si}(111)$  interface, the interface is abrupt, and  $\text{Si}^{1+}$  and  $\text{Si}^{3+}$  species dominate, as de-

scribed above. In addition, atomic force microscopic study revealed that domains with  $\text{Si}^{1+}$  and  $\text{Si}^{3+}$  were formed at the interface.<sup>19</sup> Therefore, the atomically flat  $\text{SiO}_2/\text{Si}(111)$  interface that consists only of  $\text{Si}^{1+}$  or  $\text{Si}^{3+}$  is assumed as the interface model for calculations. Figures 2(d)–2(f) show the oxygen projected density of states [O  $2p$  density of states (DOS)] for  $\text{SiO}_2$ , P3, and P1, respectively, which are calculated with the model structures illustrated on the right.

The SXE spectrum of the bulk oxide region far from the interface is well reproduced by the calculated O  $2p$  DOS for an amorphous structure, which is distorted from a cristobalite while maintaining a six-membered ring network [Figs. 2(a) and 2(d)]. The Si-O-Si angle and Si-O bond length are predominantly distributed from  $140^\circ$  to  $155^\circ$  and  $1.55 \text{ \AA}$  to  $1.65 \text{ \AA}$  in the present calculations, respectively, which is consistent with previous experimental results.<sup>20</sup> As for the P3 interface, the Si-O-Si angle is distributed from  $131.6^\circ$  to  $151.6^\circ$  and the Si-O bond length from  $1.58 \text{ \AA}$  to  $1.76 \text{ \AA}$  in the theoretically optimized structure. The local variation from the amorphous  $\text{SiO}_2$  is caused by stress, which results in the appearance of a shoulder at 4 eV and the broadening of the nonbonding state from 7.75 eV to 9.13 eV [Figs. 2(b) and 2(e)]. This implies that the P3 layer itself is about to become an amorphous state. On the other hand, for the P1 interface, the Si-O-Si angle and the Si-O bond length should be artificially maintained near  $180^\circ$  and  $1.9 \text{ \AA}$ , respectively, in order to reproduce the sharp nonbonding peak at 6.50 eV [Figs. 2(c) and 2(f)]. Thus, the valence electronic structure strongly depends on the bond angle and bond length of each atom. So far, there are many proposed models for the  $\text{SiO}_2/\text{Si}(111)$  interface. However, several models are consistent with the experimental results.<sup>8,21–24</sup> We performed calculations based on these possible models. Finally, we have found that only our present model reproduces the local valence structure observed by SXE.

Next, we investigated how the interface structures with different chemical environments affect the conduction and valence states in the interface region using the calculated models. This would enable us to understand atomic-scale transport properties of carrier. Previously Muller *et al.*<sup>12</sup> used cross-sectional EELS and succeeded in observing conduction band across the  $\text{SiO}_2/\text{Si}(100)$  interface. However, the interfacial electronic states were observed as the average and not as individual states because of the electrons passing through thick sample in transmission electron microscopy.<sup>12</sup> Figure 3 shows the calculated conduction-band minimum (CBM) and valence-band maximum (VBM) in the interface region for the  $\text{SiO}_2/\text{Si}(111)$  interface with P1 interface and the  $\text{SiO}_2/\text{Si}(111)$  interface with P3 interface. In the interface region from 0  $\text{ \AA}$  to 2  $\text{ \AA}$ , the P1 interface exhibits a similar band gap to the bulk Si, while the gap of the P3 interface gradually becomes wider. This means that since the P1 interface is relatively more conductive, the interface properties

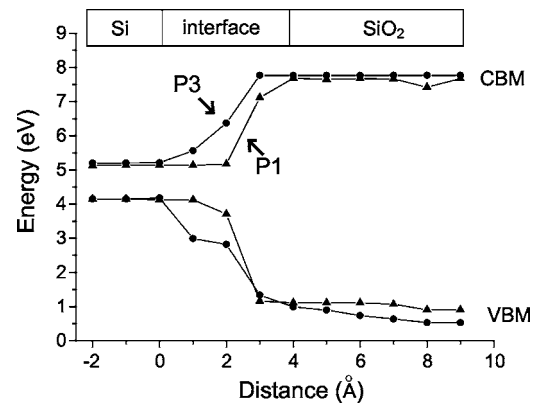


FIG. 3. Calculated energy band-gap variation in the structures with P1 and P3 along the normal direction to the interface. The position of the topmost silicon of the substrate, shown in Fig. 2, is the set to be the origin of the distance.

strongly depend on the local structures; silicon-based devices, when the gate width becomes less than 10 nm, should be affected by the suboxide composition at the interface.

In this paper, we present our approach using SXA and SXE, which successfully observes the atom-specific electronic states at the  $\text{SiO}_2/\text{Si}$  interface. In future experiments, since SXA and SXE are photo-in and photo-out processes, respectively, the measurements can be performed even when electric field, magnetic field, and high pressure are applied. The present approach is, therefore, widely applicable to the interface electronic states of various systems and will be indispensable for evaluating the atomic scale properties of interfaces of matter and designing new exotic materials.

#### IV. SUMMARY

In summary, using the  $\text{SiO}_2/\text{Si}$  interface as a prototype, we successfully observed site-specific valence electronic states at the interface by means of SXA and SXE spectroscopy. We found that the interface electronic states were noticeably different from those of bulk  $\text{SiO}_2$  and were strongly dominated by the chemical state of each atom at the interface. In addition, the comparison of the experimental results with first-principles calculations quantitatively revealed not only the Si-O-Si bond angle and Si-O bond length at the interface but also the interface electronic properties in atomic scale.

#### ACKNOWLEDGMENTS

We wish to thank Professors Hattori and Nohira for their useful discussion and gratefully acknowledge the help by Dr. Tamenori of JASRI. This work was supported by the Nanotechnology Support Project of the Ministry of Education, Culture, Sports, Science, and Technology.

- \*Author to whom correspondence should be addressed; e-mail: yyama@issp.u-tokyo.ac.jp
- <sup>1</sup>For a review, see, P. W. Anderson, in *Elementary Excitation in Solids, Molecules, and Atoms*, Part A, edited by J. A. Devreese, A. B. Kunz, and T. C. Collins (Plenum, New York, 1974), p. 1.
- <sup>2</sup>R. Arita, Y. Tanida, K. Kuroki, and H. Aoki, *Phys. Rev. B* **64**, 245112 (2001).
- <sup>3</sup>*High-Temperature Superconductivity*, edited by V. L. Ginzburg and D. A. Kirzhnits (Consultants Bureau, New York, 1982).
- <sup>4</sup>E. H. Nicollian and J. R. Brews, *MOS (Metal Oxide Semiconductor) Physics and Technology* (Wiley, New York, 1982).
- <sup>5</sup>J. Stöhr, *NEXAFS Spectroscopy* (Springer, Berlin, 1992).
- <sup>6</sup>A. Kotani and S. Shin, *Rev. Mod. Phys.* **73**, 203 (2001).
- <sup>7</sup>N. Wassdahl, A. Nilsson, T. Wiell, H. Tillborg, L. C. Duda, J. H. Guo, N. Mårtensson, J. N. Andersen, J. Nordgren, and R. Nyholm, *Phys. Rev. Lett.* **69**, 812 (1992).
- <sup>8</sup>K. Ohishi and T. Hattori, *Jpn. J. Appl. Phys., Part 2* **33**, L675 (1994).
- <sup>9</sup>T. Tokushima, Y. Harada, M. Watanabe, Y. Takata, E. Ishiguro, A. Hiraya, and S. Shin, *Surf. Rev. Lett.* **9**, 503 (2002).
- <sup>10</sup>J. Yamauchi, M. Tsukada, S. Watanabe, and O. Sugino, *Phys. Rev. B* **54**, 5586 (1996).
- <sup>11</sup>The electron inelastic-mean-free-paths were estimated using NIST Standard Reference Database 71, “NIST Electron Inelastic-Mean-Free-Path Database Ver. 1.1.”
- <sup>12</sup>D. A. Muller, T. Sorsch, F. H. Baumann, K. Evans-Lutterodt, and G. Timp, *Nature (London)* **399**, 758 (1999).
- <sup>13</sup>Z. Y. Wu, F. Jollet, and F. Seifer, *J. Phys.: Condens. Matter* **10**, 8083 (1998).
- <sup>14</sup>J. Sarnthein, A. Pasquarello, and R. Car, *Phys. Rev. Lett.* **74**, 4682 (1995).
- <sup>15</sup>F. J. Himpsel, F. R. McFeely, A. Taleb-Ibrahimi, J. A. Yarmoff, and G. Hollinger, *Phys. Rev. B* **38**, 6084 (1988).
- <sup>16</sup>Y. Yamashita, A. Asano, Y. Nishioka, and H. Kobayashi, *Phys. Rev. B* **59**, 15872 (1999).
- <sup>17</sup>D. J. Wallis, P. H. Gaskell, and R. Brydson, *J. Microsc.* **180**, 307 (1995).
- <sup>18</sup>G. Hollinger, E. Bergigna, H. Chermette, F. Himpsel, D. Lohex, M. Lannoo, and M. Bensoussan, *Philos. Mag. B* **55**, 735 (1987).
- <sup>19</sup>M. Ohashi and T. Hattori, *Jpn. J. Appl. Phys., Part 2* **36**, L397 (1997).
- <sup>20</sup>E. Dupree and R. F. Pettifer, *Nature (London)* **308**, 523 (1984).
- <sup>21</sup>M. T. Sieger, D. A. Luh, T. Miller, and T.-C. Chiang, *Phys. Rev. Lett.* **77**, 2758 (1996).
- <sup>22</sup>M. Niwano, H. Katakura, Y. Takeda, T. Takakuwa, N. Miyamoto, A. Hiraiwa, and K. Yagi, *J. Vac. Sci. Technol. A* **9**, 195 (1991).
- <sup>23</sup>T. Shimura, H. Misaki, M. Umeno, I. Takahashi, and J. Harada, *J. Cryst. Growth* **166**, 786 (1996).
- <sup>24</sup>S. Dreiner, M. Schürmann, C. Westphal, and H. Zacharias, *Phys. Rev. Lett.* **86**, 4068 (2001).